Solid State Ionics 301 (2017) 176–181

Contents lists available at ScienceDirect

Solid State Ionics

journal homepage: www.elsevier.com/locate/ssi

Energetics of metal ion adsorption on and diffusion through crown ethers: First principles study on two-dimensional electrolyte

Wei-Hua Wang [a,b,**], Cheng Gong [a], Weichao Wang [a,b], Fantai Kong [a], Hanchul Kim [a,c], Susan K. Fullerton-Shirey [d,e], Alan Seabaugh [d], Kyeongjae Cho [a,*]

[a] Department of Materials Science and Engineering, The University of Texas at Dallas, Richardson, TX 75080, USA
[b] Department of Electronics & Tianjin Key Laboratory of Photo-Electronic Thin Film Device and Technology, College of Electronic Information and Optical Engineering, Nankai University, Tianjin 300170, PR China
[c] Department of Nano Physics, Sookmyung Women's University, Seoul 140-742, Republic of Korea
[d] Department of Electrical Engineering, University of Notre Dame, Notre Dame, IN 46556, USA
[e] Department of Chemical and Petroleum Engineering, University of Pittsburgh, Pittsburgh, PA 15213, USA

ARTICLE INFO

Article history:
Received 20 July 2016
Received in revised form 28 January 2017
Accepted 31 January 2017
Available online 9 February 2017

Keywords:
Two-dimensional (2D) electrolyte
Ion adsorption
Ion diffusion
First principles calculation

ABSTRACT

Macrocyclic crown ethers (CEs) have tunable cavity sizes and site-selective binding with metal ions, making the CE-ion complex a promising candidate as a two-dimensional (2D) electrolyte. In this work, density functional theory method is used to determine the energetically stable structures of 12-crown-4 ether (CE4) and 15-crown-5 ether (CE5) complexed with four cations: Li^+, Na^+, Mg^{2+}, Ca^{2+}. In addition to the CE-ion binding energies, the diffusion barriers for ion transport through the CE cavities are calculated. Among the complexes investigated, CE5 presents the lowest energy barrier for ion diffusion. The barriers for Li^+ travelling through a single CE5 and moving between two CE5s are 0.29 eV and 0.16 eV, respectively. Field-controlled modulation of the diffusion barrier is also demonstrated. By applying a 0.15 V/Å electric field perpendicular to the plane of the CE, the diffusion barrier of Li^+ through one CE5 can be reduced from 0.29 to 0.20 eV to facilitate the ion transport.

1. Introduction

Inorganic and organic electrolytes are widely investigated for applications in energy storage [1–5], memory [6–9] and as a reconfigurable electrostatic dopant for transistors [10–12]. Although both solid and liquid electrolytes have been investigated for these applications, solid state electrolytes have several advantages over liquids, including lower flammability, chemical stability, and suppression of dendritic growth [13–16]. Thin films of inorganic solid electrolytes based on sulfides, Ge-based chalcogenides and oxides can be deposited by sputtering, atomic layer deposition or chemical vapor deposition [17], while polymer electrolytes and ionic liquids can be deposited by simple spin-coating or drop-casting [18]. For the applications mentioned above, ion mobility governs device performance. For energy storage, a minimum ionic conductivity of 10^{-3} S/cm is required to supply sufficient power density to a portable electronic device. For flash memory, ions must diffuse on the timescale of nanoseconds to provide switching speeds sufficiently high to compete with current memory technology. For electrostatic doping, the ability to reconfigure the type of dopant (*i.e.*, *p*- or *n*-type) on nanosecond timescales may enable novel devices. Polymer electrolytes have notably lagged inorganic electrolytes in their conductivity by several orders of magnitude. For example, polyethylene oxide (PEO) based electrolytes are the most widely studied, and in the absence of a plasticizer or other filler material, conductivity is limited to ~10^{-6} S/cm at room temperature [19]. In contrast, the ionic conductivity of Ge-based solid electrolytes such as $Li_{10}GeP_2S_{12}$, exceeds 10^{-2} S/cm at room temperature [1].

While solid electrolytes can be deposited as thin films (μm scale thickness), a two-dimensional (2D) electrolyte (*i.e.*, atomically or molecularly thin at nm scale) has not been reported in literatures. The development of a solid and 2D electrolyte is motivated by the continuous scaling of electronic devices to smaller dimensions. For example, transistors based on 2D semiconductors show great promise, but require doping strategies other than substitutional doping which will alter the band structure. The availability of a 2D electrolyte to electrostatically dope a 2D transistor *n*- or *p*-type with sheet carrier densities on the order of 10^{14} cm^{-2} would be valuable. Similarly, as 2D materials such as graphene are used in next generation batteries, the availability of a 2D electrolyte may enable rapid scaling [20]. However, currently available solid electrolyte materials are not suitable candidates for

* Corresponding author.
** Corresponding author at: Department of Materials Science and Engineering, The University of Texas at Dallas, Richardson, TX 75080, USA.
E-mail addresses: whwangnk@nankai.edu.cn (W.-H. Wang), kjcho@utdallas.edu (K. Cho).

http://dx.doi.org/10.1016/j.ssi.2017.01.029
0167-2738/

nanometer (nm) scale 2D electrolytes since their intrinsic surface roughness itself is larger than nm scale due to diverse atomic arrangements on electrolyte surface. From this perspective, it is evident that suitable 2D electrolyte candidate materials are required to possess intrinsic planar atomic structures with sub-nanometer thickness.

To serve as a 2D electrolyte, a molecule-ion pair must meet several requirements: 1) the molecule must solvate metal cations, 2) the molecule-ion pair must lay flat on a 2D surface with a thickness of one molecular layer, 3) the metal cation must diffuse in the direction orthogonal to the plane of the molecule, and 4) the molecule must provide a sufficiently small barrier for cation diffusion so that the requirement for fast ion mobility can be met (*e.g.*, nanosecond diffusion for the memory). In this work, we use density functional theory (DFT) method to explore the possibility of using macrocyclic crown ethers (CE) in combination with Li^+, Na^+, Mg^{2+} and Ca^{2+} cations for the development of a 2D electrolyte. CEs are chosen for their tunable cavity size and site-selective binding with metal ions [21–24]. The extent to which the CE can lay flat on a surface depends on the cavity size, which is determined by the number of oxygen atoms *n* in the general chemical formula of $(—CH_2CH_2O—)_n$. DFT calculations performed by De and co-workers reported structures and stability of seven CEs of varying size from 3-crown-1 ether (CE1) to 21-crown-7 ethers (CE7) [24]. They also reported the minimum energy configurations between Li^+/Na^+ and seven CEs from CE1 to CE7. Their results showed that CE4-ion and CE5-ion have planar configurations [24]. Most of the previous theoretical reports on this topic have focused on CE-ion stability and structure, including calculations of binding energies and minimum energy configurations of the CE-ion complex. In addition to the static binding configurations, a critical issue for the use of a CE-based 2D electrolyte in the applications outlined above is the diffusion of the ions through the cavity of the CEs. The objective of this study is to identify the most promising CE-ion complex for application as a 2D electrolyte. This is accomplished through a systematic study of the energetics of complexes formed between CE4 or CE5 and Li^+, Na^+, Mg^{2+}, Ca^{2+} cations. Owing to the high energetic stability and low ionic diffusion barrier, the results show that CE5-Li^+ complex is one promising candidate as a 2D electrolyte.

2. Theoretical methods

All the calculations are carried out using the projector augmented wave (PAW) technique [25] as implemented in the Vienna *ab initio* Simulation Package (VASP) [26,27]. The generalized gradient approximation (GGA) with the Perdew-Burke-Ernzerhof (PBE) scheme [28] and the local density approximation (LDA) [29] are adopted for the exchange-correlation function. The electron wave function is expanded in the plane wave basis set with a kinetic energy cutoff of 400 eV, and the electronic optimization stops when the total energies of neighboring optimization loops differ $<10^{-4}$ eV. The Brillouin zone integrations have been performed using only one Γ-point, similar to the cluster structure calculations [30]. During the geometry optimizations, the atomic positions are fully relaxed with a conjugate gradient (CG) method and the remnant force on each atom is converged to <0.01 eV/Å. The nudged elastic band (NEB) method [31] is adopted to calculate the energy barrier of the metal ion diffusion through the cavity of the CE molecule and between CE molecules. The remnant force on each atom is chosen to be <0.05 eV/Å in NEB calculation.

As mentioned in the introduction, cyclic CEs are comprised of $(—CH_2CH_2O—)_n$ where the cavity size depends on the number of repeated units, *n*. Even for the same number of repeated units, several CE isomers are present. For isolated CEs, previous studies showed that they are energetically more stable with ether oxygen atoms on both sides of the ring compared to those with oxygen atoms on only one side, due to the intramolecular CH-O repulsion [24]. However, when a metal cation is introduced, the configuration with all the ether oxygen atoms located on one side of the CE becomes more stable because of the strong electrostatic attraction between the cation and the ether oxygen atoms. Owing to the stability imparted by the presence of the cation, only configurations with all O atoms on the same side of the ring are considered in this study. As one promising 2D electrolyte, the practical morphology of crown ether molecules should be correlated with interaction strength between CE and the substrate. If this interaction is not strong, *i.e.* weak interaction between CE and graphene, the CEs arrangement may not be closely packed and periodic. At current stage, it is essential to estimate the diffusion ability of ions through the CE cavity and between two CEs. In our calculations, all CE-ion complexes are placed in a large cubic box with the side of 18 Å to minimize artificial interactions between periodic images and enable the application of an external electric field with potential drop in the vacuum region [32,33]. The charge states of CE-ion complexes are set up through specifying the total electron number of the system. The compensating background charge in VASP would affect the vacuum potential and the reference point of the total energies. In order to minimize this effect on the calculations of total energies, the box (18 Å × 18 Å × 18 Å) is enough large and the same box size is used for all CE-ion complexes.

3. Results and discussion

3.1. Optimized structural parameters and binding energies

The optimized structures of the CE4-Li^+ and CE5-Li^+ complexes are shown in Fig. 1. It is found that the $(—CH_2CH_2O—)_n$ rings are puckered and the metal ions prefer to bind with the O side of CEs, consistent with

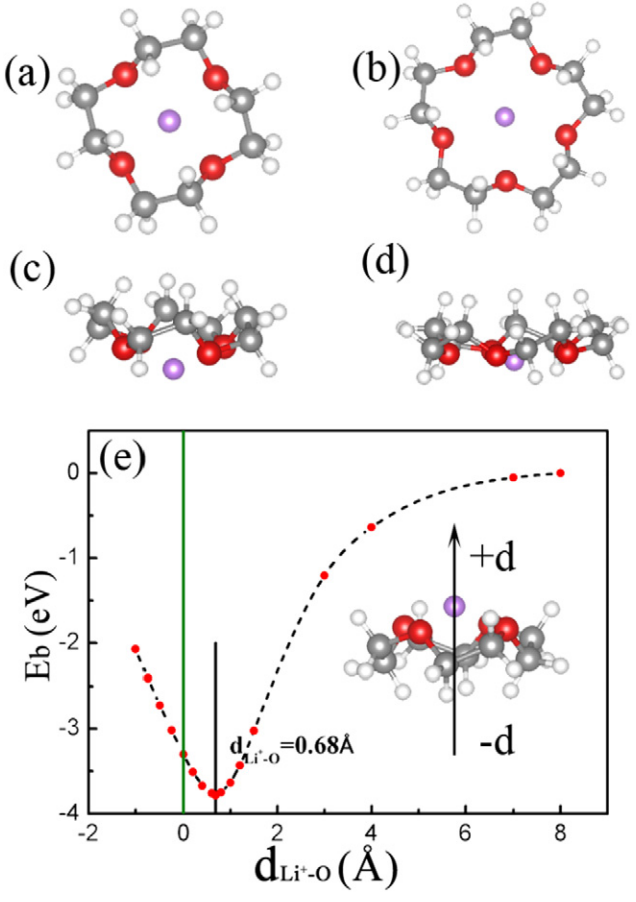

Fig. 1. Schematic structures of CE4 and CE5 binding with metal ions: (a) and (b) are top views of CE4 and CE5, respectively. (c), (d) are side views of CE4 and CE5, respectively. The dependence of the binding energy on the vertical distance of Li^+ from O plane, d_{Li^+-O}, is shown in (e) for CE4-Li^+ system. The positive value implies that the metal ion is located on the O side, while the negative value indicates the opposite side. For CE4-Li^+, the equilibrium distance is 0.68 Å.

the initial model analysis. For the same CE molecule, the relaxed structural parameters are closely correlated with the radii of ions, as shown in Table 1, where both GGA and LDA results for CE4 and CE5 are summarized. For CE4-ion complexes in Table 1(a), the cavity sizes of CE4 (r_{O-O}), the bond lengths of ion to O (r_{M-O}), and the vertical binding distances from the bound ion to O atoms plane (d_{M-O}) are listed. These structural parameters differ little (≤0.03 Å) between CE4-Li^+ and CE4-Mg^{2+} complexes because of the similar ionic radii of Li^+ and Mg^{2+}. However, for CE5 systems in Table 1(b), the bond length is elongated to 2.69 Å, and the cavity size is expanded to 2.80 Å in CE5-Na^+ complex because Na^+ is larger than Li^+. While, CE5-Mg^{2+} results in decreased cavity size and bond length down to 2.48 Å and 2.11 Å, respectively, due to a much smaller radius of Mg^{2+} than Na^+. Furthermore, compared with Mg^{2+}, Ca^{2+} (with a larger radius) forms a larger cavity size of 2.66 Å and a longer bond length of 2.36 Å between Ca^{2+} and O. On the other hand, even for the same ion Li^+, the bond length of Li^+ to O, r_{Li-O}, increases from 2.03 Å to 2.27 Å with the increase of the cavity size from CE4 to CE5. Nevertheless, the vertical binding distance, d_{Li-O}, decreases from 0.68 Å for CE4-Li^+ to 0.29 Å for CE5-Li^+. In CE4-Li^+, CE4-Mg^{2+}, CE5-Na^+ and CE5-Ca^{2+}, d_{M-O} values are all around 0.70 Å. However, CE5-Mg^{2+} is an exception. Mg^{2+} is trapped in the O atoms plane ($d_{M-O} = 0.0$ Å), and the C atoms are located at both sides of O atoms plane. This almost symmetric structure, different from the other above CE-ion systems, is speculated to be formed by a combined effect of the small Mg^{2+} radius, the large pore size of CE5 and the strong interaction between Mg^{2+} and O atoms. Due to the binding interaction overestimation with LDA exchange correlation function, the structural parameters using LDA are slightly reduced relative to those using GGA. Nonetheless, our LDA results on structural parameters are consistent with previous results based on B3LYP hybrid density functional theory [21,24].

In order to investigate the stability of the CE-ion complexes, the binding energy is calculated using the equation,

$$E_b = E_{CE-ion} - E_{CE} - E_{ion} \quad (1)$$

where $E_{CE\text{-}ion}$, E_{CE} and E_{ion} represent the total energies of CE-ion complex, CE, and metal ion, respectively. For calculation of the binding energy (E_b) of a charged defect in one solid, E_b is dependent on Fermi level (E_F) if the neutral defect is taken as the reference. While in our studied CE-ion systems, the E_b is not dependent on the E_F since the ion state is the reference in Eq. (1). Among the studied systems listed in Table 1, all the binding energies are negative, indicating that the CE-ion complexes are energetically stable. From the binding energy (E_b) curve on CE4-Li^+ shown in Fig. 1(e), E_b is around −3.80 eV at the equilibrium distance $d_{Li^+-O} = 0.68$ Å when using GGA. For comparison, LDA yields a slightly larger binding energy of about −4.00 eV, which is in agreement with the data in literatures [21,24]. It is also shown that the binding of Li^+ on O atom side of CE4 ($d_{Li^+-O} > 0$) is the only stable site. As the Li^+ ion moves to the other side of CE4 ($d_{Li^+-O} < 0$), E_b changes by a large positive value. This asymmetric binding energy profile in Fig. 1(e) is actually determined by the inherent asymmetry of CE4 molecule with O atoms residing on one side, and the strong binding interaction between metal ion and O atoms. The bond length and the interaction strength between metal ion and CE are the two key factors in determining the binding energy. For example, longer Li^+—O bond in CE5-Li^+ leads to a lower binding energy (−3.72 eV) than that (−3.80 eV) of CE4-Li^+. The divalent ions (Mg^{2+}, Ca^{2+}) have stronger interactions with O atoms than those of monovalent ions (Li^+, Na^+), inducing higher binding energies. Our binding energies of CE4-Li^+ (−3.80 eV) and CE5-Na^+ (−3.02 eV) are in good agreement with the previous studies [7]. The reports on the binding energies of CE-divalent ion complexes are still lacking in the literature, and our calculated data can provide the references for a further study.

3.2. Energy barriers of metal ions diffusion through the cavity of crown ethers

For the CE-ion complex to be used as a 2D electrolyte, fast ion diffusion through the CE is required. For example, the "switching time" for a nano-ionic memory should be on nanosecond timescales. The relationship between the switching rate and the energy barrier (E_a) can be expressed by the Arrhenius formula [34],

$$\frac{1}{\tau} \sim \nu e^{-E_a/K_B T} \quad (2)$$

where τ is the switching time, ν is the attempt frequency, and $K_B T = 25.9$ meV at the room temperature. Considering CE4-Li^+ as an example, ν can be estimated by the harmonic oscillator approximation. In the vicinity of the equilibrium point $x_0 = d_{Li^+-O} = 0.68$ Å in the binding

Table 1
The optimized structural parameters of CE-ion complex: the bond length of metal ion (M) and oxygen atoms (r_{M-O}), the distance between two nearest oxygen atoms in CE (r_{O-O}), the vertical binding distance from M to the O plane (d_{M-O}), the binding energy (E_b), and the energy barrier (E_a) for ion diffusing through the cavity of (a) CE4 and (b) CE5. The effect of a vertical electric field on E_a is also shown. For comparison, theoretical values of E_a for nanosecond switching speed are estimated using the Arrhenius formula in Eq. (2).

(a)

System	r_{M-O} (Å)	r_{O-O} (Å)	d_{M-O} (Å)	E_b (eV)	Theoretical E_a (eV)	Calculated E_a (eV)	
					~ns switching	$E = 0.0$	$E = 0.5$ (V/Å)
Li^+(GGA)	2.03	2.70	0.68	−3.80	<0.237	1.39	1.10
Li^+(LDA)	1.99	2.65	0.68	−4.00	<0.237	1.43	1.14
Mg^{2+}(GGA)	2.02	2.68	0.71	−5.29	<0.230	1.47	1.34
Mg^{2+}(LDA)	1.99	2.63	0.71	−5.83	<0.230	1.61	1.57

(b)

System	r_{M-O} (Å)	r_{O-O} (Å)	d_{M-O} (Å)	E_b (eV)	Theoretical E_a (eV)	Calculated E_a (eV)		
					~ns switching	$E = 0.0$	$E = 0.5$ (V/Å)	$E = 0.15$ (V/Å)
Li^+(GGA)	2.27	2.65	0.29	−3.72	<0.227	0.32	0.0	0.23
Li^+(LDA)	2.22	2.59	0.28	−3.89	<0.230	0.29	0.0	0.20
Na^+(GGA)	2.69	2.80	0.72	−3.02	<0.215	1.05	0.64	–
Na^+(LDA)	2.42	2.74	0.67	−3.13	<0.215	0.89	0.63	–
Mg^{2+}(GGA)	2.11	2.48	0.0	−6.31	<0.222	0.31	0.56	–
Mg^{2+}(LDA)	2.07	2.44	0.02	−6.97	<0.222	0.31	0.57	–
Ca^{2+}(GGA)	2.36	2.66	0.68	−6.63	<0.217	0.72	0.63	–
Ca^{2+}(LDA)	2.30	2.59	0.65	−7.47	<0.217	0.70	0.59	–

energy curve of Fig. 1(e), the binding energy can be approximated to a harmonic form,

$$E_B(x) = E_b(x_0) + \frac{1}{2}k(x-x_0)^2 \quad (3)$$

The spring constant k can be numerically determined from the binding energy curve. The attempt frequency $\upsilon = \sqrt{k/m}/2\pi$ is calculated to be $\upsilon \approx 9.31\times10^{12}(s^{-1})$ using the derived k and ion mass, and adopted into Eq. (2). The maximum energy barriers for all systems are calculated with the corresponding masses of ions and the calculated attempt frequencies, which are provided in Table 1. It is clearly seen that all the theoretical expectation values of E_a for nanosecond switching should be <0.24 eV for the examined CE-ion complexes.

For a specific CE-ion complex, the energy barrier for ion diffusion through the CE cavity can be calculated using the NEB method. For the ease of comparison, CE4-Li^+ is taken as the example. In Fig. 1(e), we have shown that the Li^+ ion has only one stable binding site, and it does not seem to allow the ion diffusion through the CE cavity. However, it is important to note that the CE4 configuration is asymmetric with O atoms on one side, and there is also an equivalent configuration with O atoms on the opposite side. This consideration shows that the CE4-Li^+ complex also has two equivalent asymmetric configurations (left and right models in Fig. 2(a)). Due to the strong binding between Li^+ and O atoms in CE4-Li^+,when the Li^+ moves from the O atoms side to the other side, CE4 will change its own configuration and flip the O atom sites as shown in Fig. 2(a). Thus, we can calculate the energy barrier through flipping the complex of CE4-Li^+. The typical configurations for Li^+ diffusing through the CE4 cavity are shown in Fig. 2(a). It is important to determine the transition state to obtain an accurate energy barrier. As discussed above, as long as the CE molecule is asymmetric, Li^+ will bind to the side with O atoms rather than the side with hydrocarbon (as shown in Fig. 1), and the Li^+ diffusion through the cavity of CE4 would not occur without changing the CE4 configuration simultaneously. Therefore, in the transition state shown in Fig. 2(a), the O, C atoms and Li^+ are in the same plane, and two H atoms bonding with one C atom are symmetric relative to the C and O plane, which is clearly shown in its side view. We have checked the charge states of the CE molecule and Li in the CE4-Li^+ complex based on Bader charge analysis. Regardless of distance between CE4 and Li^+, the CE4 is in the neutral state and Li always remains one positive (+1) charge state, *i.e.* Li^+. The reason is that one positively charged state is set up to simulate a CE-Li^+ complex and Li is much easier to lose its one 2*s* electron than the CE4 molecule. Thus, no charge transfer occurs between CE4 and Li^+. With Li^+ gradually approaching the O atoms plane from the initial state to the transition state, the bond length of Li to O (r_{M-O}) becomes smaller and the cavity size of CE4 (r_{O-O}) simultaneously decreases. In the transition state, r_{M-O} and r_{O-O} are 1.72 Å and 2.43 Å, respectively. A similar decrease of the bond length is also reported in Ref. [21].

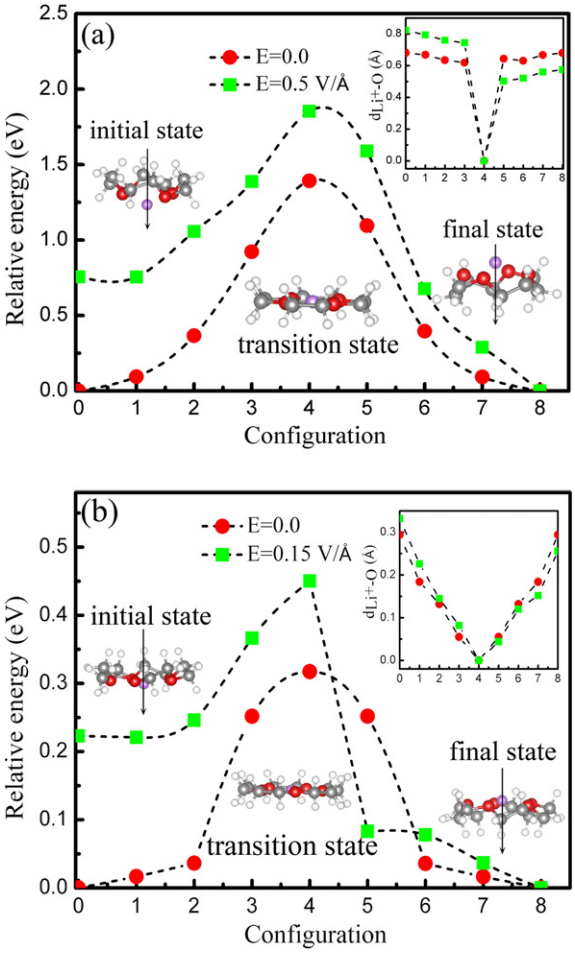

Fig. 2. Energy barrier curves of Li^+ diffusing through the cavities: (a) CE4 and (b) CE5. The energy profiles modified by a vertical electric field (pointing downward) are also presented for the field strength of 0.5 V/Å and 0.15 V/Å in (a) and (b), respectively. Inset shows the binding site of Li^+ with respect to the O atoms plane, d_{Li^+-O}, without and with electric filed. In the whole diffusion process, Li^+ is always located at the O side, resulting in positive d_{Li^+-O}. The initial state, the transition state, and the final state of Li^+ diffusion through CE4 or CE5 are also shown. In this process of diffusion, the CE molecule flips following the motion of Li^+. In the transition state, all the O and C atoms are located in the same plane. The two H atoms bonding with a C atom are symmetric relative to the C and O plane.

Fig. 2(a) shows the energy barrier (E_a) of Li^+ diffusing through the cavity of CE4. E_a of CE4-Li^+ is 1.39 eV using GGA, which is too large to meet the requirement of a fast switching speed of nanoseconds. In the absence of an external electric field, the geometrical structures of initial and final CE4-Li^+ configurations are mirror symmetric relative to the intermediate transition configuration, and thus the calculated energy barrier curve is also symmetric. To meet the fast switching speed, the energy barrier needs to be lowered. A vertical external electric field of $E = 0.5$ V/Å is applied to examine the field effect to modulate the geometrical structures and the energy barrier. Under this condition, the energy barrier curve is asymmetric because the initial and final states are not symmetric relative to the transition state, which can also be deduced from the vertical binding distance (d_{M-O}) of the inset in Fig. 2(a). The reason is that the electric field direction is from CE4 to Li^+ for 0–3 configurations and from Li^+ to CE4 for 5–8 configurations. In the former configurations, a downward electrostatic force acts on Li^+ in Fig. 2(a). To get to the new equilibrium position, Li^+ tends to displace away from CE4 and the binding distance is elongated. Conversely, the electrostatic force on Li^+ is pointing to CE4 in the latter configurations. To keep the stabilized state, the binding distance is shortened. After applying this electric field, E_a is reduced to 1.10 eV, which is still too large to achieve the fast switching. Based on these findings, it is necessary to look into other CE-ion complexes and identify which one possesses a small E_a around 0.24 eV. For CE-Li^+ complexes, Li^+ is easier to pass through the CE molecules with larger cavity, and the CE5-Li^+ is possibly a better candidate than CE4-Li^+. On the other hand, even larger CE molecules may not be a good candidate considering non-planar configurations of such large molecules. From DFT calculations, CE5-Li^+ shows E_a value of as small as 0.32 eV (0.29 eV) using GGA (LDA). Furthermore, E_a can be reduced to 0.23 eV (0.20 eV) using GGA (LDA) in the presence of a small vertical electric field of 0.15 V/Å, as shown in Fig. 2(b).

The energy barriers from GGA and LDA calculations for all systems of CE4-ion and CE5-ion are listed in Table 1. In Table 1(a), due to the stronger interaction between Mg^{2+} and O atoms, E_a of CE4-Mg^{2+} is as large as 1.47 eV. The field reduction effect on E_a with an external electric field of 0.5 V/Å is not sufficient. For CE5-ion complexes in Table 1(b), the Na^+ and Ca^{2+} (with larger ion radii than Li^+ and stronger binding interaction with O atoms) have E_a up to 1.05 eV for CE5-Na^+ and 0.72 eV for

CE5-Ca^{2+} using GGA. Under the electric field of 0.5 V/Å, the E_a would be reduced to 0.6 eV, which still does not meet the fast switching requirement. The radius of Mg^{2+} is close to that of Li^+, and E_a is as small as 0.31 eV for Mg^{2+} diffusing through CE5. However, it is worthwhile to note that E_a is increased regardless of the upward or downward direction of electric field, indicating the absence of the field-assisted reduction effect. As discussed in Section 3.1, the relaxed initial state of CE5-Mg^{2+} is nearly symmetric. An external electric field will push Mg^{2+} away from the plane of O atoms, resulting in an asymmetric structure. Under the influence of the electric field, the diffusion of Mg^{2+} through the cavity of CE5 becomes more difficult and E_a increases rather than achieves field-induced barrier reduction.

Among all the CE-ion systems in Table 1, E_a of CE5-Li^+ is relatively as small as 0.29 eV and it can be further reduced to 0.20 eV under $E =$ 0.15 V/Å. Therefore, CE5-Li^+ is the most promising system to realize the fast switching speed for application as a 2D electrolyte.

3.3. Energy barriers of Li^+ diffusion between two crown-5 ethers

In a practical device design, a 2D electrolyte with several molecular layers (rather than single CE-ion layer) may be required to reduce leakage current. Thus, it is also important to consider ion binding and diffusion between two CE molecules within a stacked configuration. A side view of two CE5 molecules interacting with one Li^+ ion is illustrated schematically in the inset of Fig. 3. The distance between two CE5 molecules is labeled by the separation distance of O planes, d_{O-O}. To determine the optimal CE5-CE5 distance, the total energy is calculated as a function of d_{O-O}. As d_{O-O} increases, the total energy decreases initially and then increases; however, the binding site of Li^+ with respect to the plane of the bottom O atoms, d_{Li^+-O}, monotonically decreases toward the value of an isolated CE5-Li^+ system. The structure of the most stable configuration is shown in the inset of Fig. 3 with $d_{O-O} =$ 3.2 Å and $d_{Li^+-O} = 0.64$ Å. The vertical binding distance from Li^+ to the bottom CE5 (d_{Li^+-O}) is significantly larger than that of 0.28 Å in an isolated CE5-Li^+ system. This increase of the binding distance indicates a stronger binding interaction between Li^+ with the bottom CE5 and a weaker interaction with top CE5 rather than an equivalent binding between Li^+ and two CE5 molecules. However, apart from the binding of Li^+ with the bottom CE5, the binding of Li^+ with the top CE5 is also significant. With the decrease of d_{O-O} from equilibrium distance of 3.2 Å, the Li^+ moves away from the bottom CE5 and approaches to the middle of two CE5 molecules. Such interaction of the Li^+ ion with both CE5 molecules would facilitate the inter-molecular ion transport.

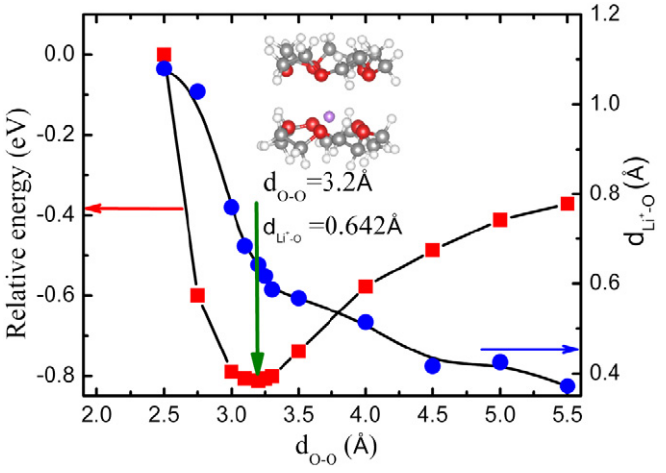

Fig. 3. Total energy (E_t, left axis) and the vertical binding site (d_{Li^+-O}, right axis) as functions of the distance between two CE5 molecules (d_{O-O}) in one Li^+ and two CE5 molecules system. In the most energetically favorable state, the inter-molecular separation (d_{O-O}) is 3.2 Å and the distance from Li^+ to the O plane of the bottom CE5 (d_{Li^+-O}) is 0.642 Å.

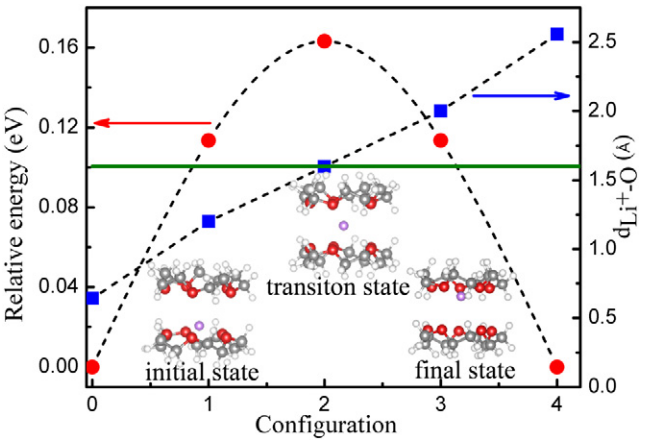

Fig. 4. The energy barrier curve (left axis) of Li^+ diffusion between two CE5 molecules and the vertical distance (right axis) of the Li^+ binding site away from the O plane of the lower CE5, d_{Li-O}. The schematic structures of Li^+ diffusing between two CE5 molecules are inserted. Initially, Li^+ is close to the bottom CE5, then it moves into the middle location in the transition state, and finally it arrives at the binding site close to the top CE5.

Nevertheless, with the separation distance d_{O-O} increasing, the influence of the top CE5 on the interaction of the bottom CE5-Li^+ becomes weaker, which results in a gradually decreased binding site d_{Li^+-O} and a much stronger binding interaction of the bottom CE5-Li^+. For non-ideal stacking of CE5 molecules, the ion transport would become correspondingly more difficult due to larger inter-molecular stacking distance. Further, when more Li^+ ions are involved in the system, the energy barrier would be larger owing to the Coulomb repulsion between Li^+ ions.

The diffusion barrier (E_a) of Li^+ between two CE5 molecules is also calculated using the NEB method. The important configurations during the diffusion process are also shown in Fig. 4. The detailed binding distance and the energy barriers are shown by the curves in Fig. 4. Initially, Li^+ is close to the bottom CE5 in the initial state with $d_{Li^+-O} = 0.64$ Å. During the inter-molecular transport, it moves to the middle location with $d_{Li^+-O} = 1.6$ Å, and it further moves to bind closely to the top CE5 with $d_{Li^+-O} = 2.56$ Å in the final state. The energy barrier for Li^+ diffusion from the bottom CE5 to the top CE5 is 0.16 eV, which is smaller than the barrier for intra-molecular transport through CE5 cavity, 0.29 eV. These small energy barriers for ion transport through CE5 and between CE5 molecules might indicate a fast ion transport through multi-layer CE stacks and consequently a high speed switching.

4. Conclusion

In this study, we have examined the binding energies of metal ions (Li^+, Na^+, Mg^{2+}, Ca^{2+}) with CE molecules and the energy barriers to ion diffusion through the cavities of CEs and between two CE molecules, which are shown to depend on the radii of ions, the cavity sizes of CE molecules, and the interaction strengths between ions and O atoms. Among all the studied systems of metal ions interacting with CEs, the energy barrier for Li^+ diffusion through single CE5 and between two CE5 molecules are found to be around 0.29 eV and 0.16 eV, respectively. A small vertical electric field ($E = 0.15$ V/Å) is shown to facilitate Li^+ travelling through the cavity of CE5 with a lowered barrier of 0.20 eV, which meets the requirement of a fast switching speed of nanoseconds. Therefore, the CE5-Li^+ complex is proposed to be one candidate 2D electrolyte in application for nanosecond ionic switching devices.

Acknowledgements

One of the authors (W. H. Wang) would like to thank Dr. F. Gao and Dr. X. H. Zheng from Chinese Academy of Sciences for the fruitful discussions. This work is supported in part by the National Key Research and

Development Program of China with No 2016YFB0901600 and by the Center for Low Energy Systems Technology (LEAST), one of six centers of STARnet, a Semiconductor Research Corporation program sponsored by MARCO and DARPA. The support from NSFC (Nos. 11104148, 11404172 and 21573117) is also acknowledged. H.K. acknowledges the support by the NRF grant funded by the Korean government (MSIP) (No. 2015R1A2A2A01005564). Parts of the calculations were performed at the Texas Advanced Computing Center (TACC) in Austin (http://www.tacc.utexas.edu).

References

[1] N. Kamaya, K. Homma, Y. Yamakawa, M. Hirayama, R. Kanno, M. Yonemura, T. Kamiyama, Y. Kato, S. Hama, K. Kawamoto, A. Mitsui, Nat. Mater. 10 (2011) 682.
[2] E. Quartarone, P. Mustarelli, Chem. Soc. Rev. 40 (2011) 2525.
[3] F. Croce, G.B. Appetecchi, L. Persi, B. Scrosati, Nature 394 (1998) 456.
[4] J.-H. Shin, W.A. Henderson, S. Passerini, Electrochem. Commun. 5 (2003) 1016.
[5] T. Inada, T. Kobayashi, N. Sonoyama, A. Yamada, S. Kondo, M. Nagao, R. Kanno, J. Power Sources 194 (2009) 1085.
[6] R. Waser, M. Aono, Nat. Mater. 6 (2007) 833.
[7] S. Wu, T. Tsuruoka, K. Terabe, T. Hasegawa, J.P. Hill, K. Ariga, M. Aono, Adv. Funct. Mater. 21 (2011) 93.
[8] M.N. Kozicki, C. Gopalan, M. Balakrishnan, M. Park, M. Mitkova, Non-volatile Memory Based on Solid Electrolytes: Non-volatile Memory Technology Symposium, Orlando, Florida, 15–17 November 2004 10–17.
[9] A. Chen, Ionic Memories: Status and Challenges: 9th Annual Non-volatile Memory Technology Symposium, Pacific Grove, California, November 11–14, 2008 27–31.
[10] Y.J. Zhang, J.T. Ye, Y. Yomogida, T. Takenobu, Y. Iwasa, Nano Lett. 13 (2013) 3023.
[11] S.H. Kim, K. Hong, W. Xie, K.H. Lee, S. Zhang, T.P. Lodge, C.D. Frisbie, Adv. Mater. 25 (2013) 1822.
[12] B.Y. Xia, W. Zhang, M. Ha, J.H. Cho, M.J. Renn, C.H. Kim, C.D. Frisbie, Adv. Funct. Mater. 20 (2010) 587.
[13] M. Marcinek, J. Syzdek, M. Marczewski, M. Piszcz, L. Niedzicki, M. Kalita, A. Plewa-Marczewska, A. Bitner, P. Wieczorek, T. Trzeciak, M. Kasprzyk, P. Lezak, Z. Zukowska, A. Zalewska, W. Wieczorek, Solid State Ionics 276 (2015) 107.
[14] S. K.C., K. Xiong, R.C. Longo, K. Cho, J. Power Sources 244 (2013) 136.
[15] S. K.C., R.C. Longo, K. Xiong, K. Cho, Solid State Ionics 261 (2014) 100.
[16] K. Xiong, R.C. Longo, S. K.C., W. Wang, K. Cho, Comput. Mater. Sci. 90 (2014) 44.
[17] J.B. Bates, N.J. Dudney, G.R. Gruzalski, R.A. Zuhr, A. Choudhury, D.F. Luck, J.D. Robertson, Solid State Ionics 53 (1992) 647.
[18] K. Norrman, A. Ghanbari-Siahkali, N.B. Larsen, Annu. Rep. Prog. Chem., Sect. C: Phys. Chem. 101 (2005) 174.
[19] J.-M. Tarascon, M. Armand, Nature 414 (2001) 359.
[20] S.K. Fullerton-Shirey, A. Seabaugh, US patent application 14/213,310 (14 March 2014).
[21] A. Datta, J. Phys. Chem. C113 (2009) 3339.
[22] J.D. Rodriguez, J.M. Lisy, J. Am. Chem. Soc. 133 (2011) 11136.
[23] B. Martínez-Haya, P. Hurtado, A.R. Hortal, S. Hamad, J.D. Steill, J. Oomens, J. Phys. Chem. A 114 (2010) 7048.
[24] S. De, A. Boda, S.M. Ali, J. Mol. Struct. (THEOCHEM) 941 (2010) 90.
[25] P.E. Blochl, Phys. Rev. B 50 (1994) 17953.
[26] G. Kresse, J. Hafner, Phys. Rev. B 47 (1993) 558.
[27] G. Kresse, J. Furthmüller, Comput. Mater. Sci. 6 (1996) 15.
[28] J.P. Perdew, K. Burke, M. Ernzerhof, Phys. Rev. Lett. 77 (1996) 3865.
[29] D.M. Ceperley, B.J. Alder, Phys. Rev. Lett. 45 (1980) 566.
[30] K. Pradhan, P. Sen, J.U. Reveles, S.N. Khanna, J. Phys. Condens. Matter 20 (2008) 25524.
[31] G. Henkelman, B.P. Uberuaga, H.H. Jónsson, J. Chem. Phys. 113 (2000) 9901.
[32] C. Gong, G. Lee, B. Shan, E.M. Vogel, R.M. Wallace, K. Cho, J. Appl. Phys. 108 (2010) 123711.
[33] J. Neugebauer, M. Scheffler, Phys. Rev. B 46 (1992) 16067.
[34] K.J. Laidler, Chemical Kinetics, third ed. Harper & Row, New York, 1987 42.